Polymer 50 (2009) 1187–1196

Contents lists available at ScienceDirect

Polymer

journal homepage: www.elsevier.com/locate/polymer

Phase behaviors of comb-like liquid crystalline polysiloxanes containing fluorinated mesogenic units

Fan-Bao Meng*, Yui Cui, Hai-Bin Chen, Bao-Yan Zhang*, Chao Jia

The Research Centre for Molecular Science and Engineering, Northeastern University, Shenyang 110004, PR China

ARTICLE INFO

Article history:
Received 27 August 2008
Received in revised form
19 December 2008
Accepted 8 January 2009
Available online 14 January 2009

Keywords:
Liquid crystalline polymers
Fluoropolymers
Phase behavior

ABSTRACT

Several liquid crystalline polysiloxanes (**Pa**–**Pf**) bearing fluorinated mesogenic units were synthesized using poly(methylhydrogeno)siloxane, 4′-(4-undec-10-enoyloxy-benzoyloxy)-biphenyl-4-yl 4-fluoro-benzoate and 4′-propionyloxy-biphenyl-4-yl 4-allyloxy-benzoate, and effect of fluorinated mesogenic units on phase behaviors of the fluorinated LC polysiloxanes was studied as well. The samples **Pa** and **Pb** showed single nematic mesophase when they were heated and cooled, but **Pc**, **Pd**, **Pe** and **Pf** exhibited both smectic and nematic phases. The glass transition temperature and smectic A–nematic mesophase transition temperature of polymers increased slightly with increase of fluorinated units in the polymer systems, but mesophase–isotropic phase transition temperature decreased slightly. In XRD curves, the intensity of sharp reflections at low angle increased with increase of fluorinated mesogenic units in the polymers' systems, indicating that the longer spacer and the fluorophobic effect of fluorinated mesogenic units could lead to a significant stabilization and even to modifications of smectic mesophases.

1. Introduction

Thermotropic liquid crystalline polymers (LCPs) have unique combined properties of both liquid crystal and conventional thermoplastics, as shown by their anisotropic mechanical properties, excellent thermal stability and chemical resistance. Side-chain liquid crystalline polymers (SCLCPs) have been the subject of much interest, for both fundamental and applied reasons. Since they present an original architecture, they can potentially display interesting new structures on one hand, while on the other hand, they are expected to exhibit properties that can lead to new applications.

Recently, the use of organo-fluorine compounds has generated much research effort [1–3]. The replacement of one or several hydrogen atoms by fluorine confers to the resulting material unusual and peculiar properties which allow their use as good precursors with many applications: surface coating, fire retardants, biomedicine, etc [4]. From these, a lot of researches have been carried out on mono- or poly-fluorinated compounds having liquid crystal (LC) character. Initial studies on fluorinated liquid crystals focused on partly fluorinated alkanes [5–7]. The formation of liquid crystalline mesophases was presumably due to the strong phase separation of fluorocarbon from hydrocarbon chain segments and also to the rigid-rodlike nature of the fluorocarbon chains which tend to adopt a helical conformation in the mesophase state [8]. These kinds of fluorinated molecules may be regarded as unconventional mesogens in that they do not possess the usual molecular features of more traditional liquid crystals. Later synthetic efforts resulted in a lot of fluorinated traditional liquid crystals. The traditional liquid crystal molecules are typified by rigid core structures composed of two or more aromatic or cyclo-aliphatic rings, or combinations of them, that are either directly linked together or interconnected by bridging groups. Alkyl tails are also normally attached at both ends of the mesogenic core to introduce flexibility in the molecule and help to tailor the mesophase transitions and properties of the materials. For fluorinated traditional liquid crystals, the fluorine atoms were introduced on alkyl tails to form (semi-) perfluorinated chains [9], on the rigid cores [10] on the bridging groups [11], or in the chiral centers [12]. And much attention has been paid in nematogen design based on fluorinated systems because they have low conductivities and viscosities. In addition, because of the strong dipole moment of the C–F bond, arenes with terminal or lateral fluorine substituents are well suited for achieving a strongly dielectric anisotropy. Therefore, the controlled choice of the position of fluoro-substituents allows tailoring of appropriate dielectric anisotropies for commercial applications [4].

* Corresponding authors. Tel./fax: +86 24 83687671.
E-mail addresses: fanbaomeng@hotmail.com (F.-B. Meng), byzcong@163.com (B.-Y. Zhang).

0032-3861/$ – see front matter © 2009 Elsevier Ltd. All rights reserved.
doi:10.1016/j.polymer.2009.01.005

Fluorinated SCLCPs are a relatively new class of fluoropolymers with many interesting properties due to fluorine's small size, large electronegativity, low polarizability, and large fluorine–fluorine repulsion [13–19]. Some development of liquid crystalline polymers without conventional mesogenic units has occurred in the variation on length of the fluorinated tail [20–22]. More synthetic efforts have been focused on combination of conventional mesogenic units with partly fluorinated tails in polymeric liquid crystals [23–25]. For these kinds of fluorinated SCLCPs, the effects of position, length of fluorinated tails on the mesomorphic properties of polymers were studied thoroughly [26–28]. Although it is important in commercial applications for small molecule liquid crystals with fluorinated mesogenic units, only a limited number of fluorine-containing SCLCPs bearing fluorinated mesogenic units were reported. The purpose of this study is to investigate the effect of fluorinated mesogenic units on the mesomorphic properties of fluorinated SLCPs.

2. Experimental

2.1. Materials

4-Hydroxybenzoic acid, 4-fluoro-benzoic acid, biphenyl-4,4′-diol, bromopropene, undec-10-enoic acid, propionic acid, poly (methylhydrogeno)siloxane (PMHS) ($M_n = 2270$) and hexachloroplatinic acid hydrate were obtained from Jilin Chemical Industry Company and used without any further purification. Pyridine, thionyl chloride, toluene, ethanol, acetone, chloroform, tetrahydrofuran (THF) and methanol were purchased from Shenyang Chemical Co. Pyridine was purified by distillation over KOH and NaH before using. Toluene was used in the hydrosilylation reaction over sodium and then distilled under nitrogen.

2.2. Synthesis of 4′-(4-undec-10-enoyloxy-benzoyloxy)-biphenyl-4-yl 4-fluoro-benzoate (*M1*)

The synthetic route of monomer **M1** is shown in Fig. 1. The intermediate product 4-undec-10-enoyloxy-benzoyl chloride (**1**) was synthesized according to previous reports [29].

To a solution of biphenyl-4,4′-diol (400 mmol, 74.4 g), pyridine (18.0 mL) and 250 mL of dry THF were added dropwise to compound **1** (80 mmol, 25.8 g) at 25 °C. The mixture was stirred at room temperature under dry air for 4 h, refluxed for 18 h, and poured into 1000 mL of ice water. 17.0 g of white solid 4′-hydroxy-biphenyl-4-yl 4-undec-10-enoyloxy-benzoate (**2**) was obtained after several recrystallizations from acetone (yield: 45%), mp 176–178 °C.

4-Fluoro-benzoic acid (100 mmol, 14.0 g), and thionyl chloride (210 mmol, 25.0 g) were added into a round flask equipped with an absorption instrument of hydrogen chloride. The mixture was stirred at room temperature for 2 h, then heated to 60 °C and kept for 3 h in a water bath to ensure that the reaction finished. The mixture was distilled under reduced pressure to obtain 10.7 g of 4-fluoro-benzoyl chloride (**3**) at 190–200 °C/20 mmHg in the yield of 68%. Compound **2** (30 mmol, 14.2 g) and pyridine (1.0 mL) were dissolved in 50.0 mL of dry THF to form a solution. Compound **3** (35 mmol, 5.5 g) was added dropwise to the solution and refluxed for 16 h. The mixture was cooled, and poured in 500 mL of cold water. The precipitated crude product was filtered and recrystallized from ethanol and dried overnight at 85 °C under vacuum to obtain a white powder of product **M1** in the yield of 70%. mp: 110 °C. ^{1}H NMR ($CDCl_3$): δ (ppm) = 1.29–1.36 (10H, m, CH_2=$CHCH_2$($C\underline{H}_2$)$_5$–); 1.73–1.78 (2H, m, –$C\underline{H}_2CH_2COO$–); 2.02–2.06 (2H, m, $C\underline{H}_2$=$CHC\underline{H}_2$–); 2.37–2.60 (2H, m, –$CH_2C\underline{H}_2COO$–); 4.85–5.02 (2H, m, $C\underline{H}_2$=CH–); 5.77–5.86 (1H, m, CH_2=$C\underline{H}$–); 6.84–8.26 (16H, m, Ar–H). FT IR (KBr,): ν (cm^{-1}) = 3077, 2922, 2850 (C–H aliphatic), 1761–1705 (C=O in different ester linkages), 1605, 1508 (Ar), 1257 (C–F). Elem. Anal. Calcd. for $C_{37}H_{35}FO_6$: C, 74.73; H, 5.93; F, 3.19; O, 16.14. Found: C, 74.65; H, 5.89; F, 3.18; O, 16.17.

2.3. Synthesis of 4′-propionyloxy-biphenyl-4-yl 4-allyloxy-benzoate (*M2*)

The synthetic route of monomer **M2** is shown in Fig. 1. The intermediate product 4-allyloxy-benzoyl chloride (**4**) was synthesized according to previous reports [30].

To a solution of biphenyl-4,4′-diol (200 mmol, 37.2 g), pyridine (10.0 mL) and 120 mL of dry THF were added dropwise to compound **4** (40 mmol, 7.8 g) at 25 °C. The mixture was stirred at room temperature under dry air for 3 h, refluxed for 16 h, and poured into 800 mL of ice water. 9.7 g of white solid 4′-hydroxy-biphenyl-4-yl 4-allyloxy-benzoate (**5**) was obtained after several recrystallizations from acetone (yield: 70%), mp 182–184 °C.

Propionic acid (200 mmol, 14.8 g), and thionyl chloride (420 mmol, 50.0 g) were added into a round flask equipped with an absorption instrument of hydrogen chloride. The mixture was stirred at room temperature for 2 h, then heated to 60 °C and kept for 3 h. The mixture was distilled under reduced pressure to obtain 12.9 g of propionyl chloride (**6**) at 78 °C in the yield of 70%. Compound **5** (30 mmol, 10.4 g) and pyridine (1.0 mL) were dissolved in 50.0 mL of dry THF to form a solution. Compound **6** (40 mmol, 3.7 g) was added dropwise to the solution and refluxed for 18 h. The mixture was cooled, and poured in 200 mL of cold water. The precipitated crude product was filtered and recrystallized from acetone and dried overnight at 85 °C under vacuum to obtain a white powder of **M2** in the yield of 78%. mp: 204 °C. ^{1}H

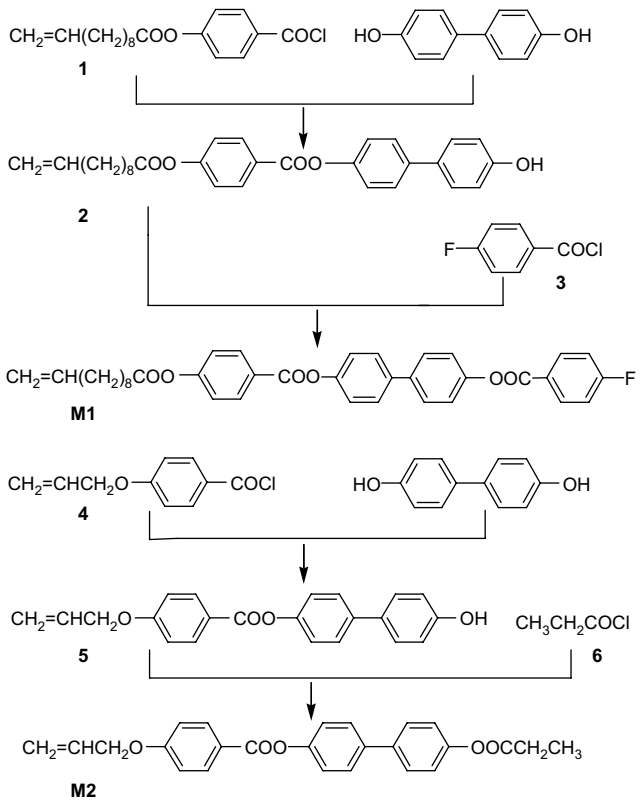

Fig. 1. Synthetic route of monomers 4′-(4-undec-10-enoyloxy-benzoyloxy)-biphenyl-4-yl 4-fluoro-benzoate (**M1**) and 4′-propionyloxy-biphenyl-4-yl 4-allyloxy-benzoate (**M2**).

NMR ($CDCl_3$): δ (ppm) = 1.19–1.24 (3H, m, –OOCCH$_2$C$\underline{H}_3$); 2.00–2.08 (2H, m, –OOC$\underline{H}_2$CH$_3$); 4.02–4.04 (2H, m, CH$_2$=CHC$\underline{H}_2$–); 5.28–5.44 (2H, m, C$\underline{H}_2$=CHCH$_2$–); 6.09–6.19 (1H, m, CH$_2$=C$\underline{H}$CH$_2$–); 6.93–8.47 (12H, m, Ar–$\underline{H}$). FT IR (KBr,): ν (cm^{-1}) = 2954, 2924, 2849 (C–H aliphatic), 1760–1708 (C=O in different ester linkages), 1608, 1509 (Ar). Elem. Anal. Calcd. for $C_{25}H_{22}O_5$: C, 74.61; H, 5.51; O, 19.88. Found: C, 74.65; H, 5.45; O, 19.81.

2.4. Synthesis of polymers

For synthesis of polymers **Pa**–**Pf**, the same method was adopted, and the synthetic route and the molecular formula of fluorinated mesogens are shown in Fig. 2. The polymerization experiments are summarized in Table 1. The synthesis of polymer **Pd** was given as an example. Fluorinated liquid crystalline monomer **M1** (2.49 g, 4.2 mmol) was dissolved in 30 mL of dry, fresh distilled toluene. To the stirred solution, LC monomer **M2** (1.13 g, 2.8 mmol), PMHS (0.41 g, 0.18 mmol) and 2 mL of a 0.5% solution of hexachloroplatinic acid in THF were added and heated under nitrogen and anhydrous conditions at 65–68 °C for 30 h. Then the mixture was cooled and poured into 120 mL methanol, and the resulting mixture was stirred for 1 h. The product was filtered off, dissolved in chloroform and precipitated in methanol (3 times), and dried at 80 °C under vacuum for 24 h to obtain 3.24 g of polymer **Pd**. ^{1}H NMR ($CDCl_3$): δ (ppm) = 0–0.36 (m, 3.35H, Si–C$\underline{H}_3$); 0.47–0.68 (m, 2.53H, Si–C$\underline{H}_2$–); 0.91–1.07 (t, 1.43H, alkyl –CH$_3$); 1.22–2.48 (m, 13.39H, alkyl –C$\underline{H}_2$–); 4.81–4.94 (m, 1.00H, –OC$\underline{H}_2$–); 6.69–8.42 (m, 17.22H, Ar–$\underline{H}$). FT IR (KBr): ν (cm^{-1}) = 2923, 2851 (C–H aliphatic), 1760–1705 (C=O in different ester linkages), 1605, 1508 (Ar), 1271 (C–F), 1154–1011 (Si–O). Elem. Anal. Found: C, 66.53; H, 6.01; F, 1.75.

2.5. Characterization

^{1}H NMR (300 MHz) spectrum was obtained with a Varian Gemini 300 NMR Spectrometer (Varian Associates, Palo Alto, CA) with tetramethylsilane (TMS) as an internal standard. The element analysis (EA) of monomers and polymers was carried out by use of an Elementar Vario EL III (Elementar, Germany). FTIR spectra of the synthesized polymers and monomers were obtained by the KBr method performed on PerkinElmer instruments Spectrum One Spectrometer (PerkinElmer, Foster City, CA). Thermal transition properties were characterized by a NETZSCH instruments DSC 204 (Netzsch, Wittelsbacherstr, Germany) at a heating rate of 10 °C min^{-1} under nitrogen atmosphere. The thermal stability of the polymers under atmosphere was measured with a NETZSCH TGA 209C thermogravimetric analyzer. X-ray diffraction (XRD) measurements of the samples were performed using Cu Kα (λ = 1.542 Å) radiation monochromatized with a Rigaku DMAX-3A X-ray diffractometer (Rigaku, Japan). The samples were heated above the clearing point to erase any previous thermal history, cooled, and then heated to the desired temperatures (100 °C for all the samples), finally quenched for measurement. Polarizing optical microscopic (POM) observation of liquid crystalline transitions and optical textures was made using a Leica DMRX (Leica, Wetzlar, Germany) microscope with crossed polarizers and equipped with a Linkam THMSE-600 (Linkam, Surrey, England) hot stage.

3. Results and discussion

3.1. Synthesis

The chemical structures of monomers **M1** and **M2** were characterized by use of FTIR and ^{1}H NMR spectra, suggesting that they are in good agreement with the prediction. Furthermore, the purity of the monomers is high, which was confirmed by EA.

Polymers **Pa**–**Pf** were synthesized via hydrosilylation reaction between Si–H groups of PMHS and olefinic C=C of the monomers. The PMHS was reacted with the olefins (10% in excess versus Si–H groups) in a minimum volume of anhydrous toluene under nitrogen. The catalyst used was hexachloroplatinic acid in THF solution. This catalyst, used in high concentration, above 65 °C for 30 h, gave good results. Reaction kinetics were followed by ^{1}H NMR and FTIR spectroscopies [31]. In the NMR spectra, the decrease of the peak near 4.68 ppm is followed, and in FTIR the decrease of the absorption band at 2160 cm^{-1} (characteristic of the Si–H function) was observed during the reaction. When the Si–H bond was disappeared absolutely, the reaction mixture was cooled and poured into methanol to obtain crude polysiloxanes. Polymers were systematically purified by several precipitations from methanol out of chloroform solutions. At last the polymers were dried under vacuum at 80 °C under vacuum for 24 h.

All the polymers were characterized by use of FTIR, ^{1}H NMR and EA. The characteristic absorption bands of representative polymer **Pd** in FTIR spectra are as follows: 2923–2851 cm^{-1} (C–H stretching), 1760–1705 cm^{-1} (C=O stretching), 1605 and 1508 cm^{-1} (C=C stretching of aromatic nucleus), 1271 cm^{-1} (C–F stretching), and 1154–1011 (Si–O stretching). Both the disappearance of Si–H stretching in the PMHS at 2160 cm^{-1} and the appearance of characteristic absorption bands of corresponding monomers suggested

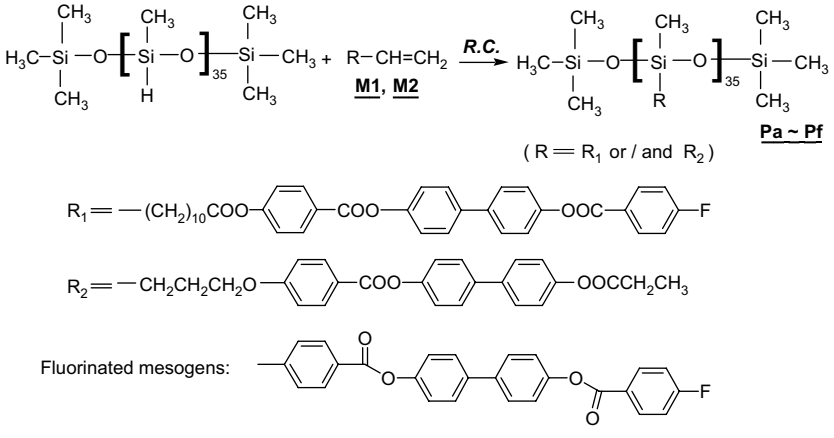

Fig. 2. Synthetic route of polysiloxanes **Pa**–**Pf**. Reagents and conditions (R.C.): H2PtCl6/tetrahydrofuran, 65 °C.

Table 1
Polymerization, analyses and X-ray data of the side-chain polysiloxanes.

Sample	Feed			F[a] (%)	Fluorinated mesogens[b] (%)	Polymer composition[c]			*d*-Spacing[d] (Å)	
	PMHS (mmol)	**M1** (mmol)	**M2** (mmol)			V_1 (%)	V_2 (%)	M_n		
Pa	0.18	0	7.0	0	0	0	100	16,300	–	4.37
Pb	0.18	1.4	5.6	0.67	16.2	21	79	17,600	–	4.34
Pc	0.18	2.8	4.2	1.25	30.2	42	58	19,000	35.20	4.35
Pd	0.18	4.2	2.8	1.75	42.3	61	39	20,300	35.14	4.33
Pe	0.18	5.6	1.4	2.19	52.9	82	18	21,700	35.26	4.35
Pf	0.18	7.0	0	2.58	62.4	100	0	23,000	35.34	4.34

[a] Mass percentage of fluorine atom in the polymer systems, obtained from element analysis of the polymers.
[b] Mass percentage of fluorinated mesogens in the polymers, calculated according to the mass percentage of fluorine atom in the polymer systems.
[c] Calculated from ^{1}H NMR spectra. $\boldsymbol{V_1}$ and $\boldsymbol{V_2}$ represent the mole fraction of **M1** and **M2** components in all the side-chains of polysiloxanes, respectively.
[d] X-ray diffraction (XRD) peaks of quenched samples after the polymers were heated at 100 °C.

the successful incorporation of monomers onto the polysiloxane chains for all the LC polysiloxanes.

For the LC polysiloxanes, it is necessary to know the polymer composition and molecular weights. NMR studies of the polymers allowed the evaluation of the grafting yield and the purity of the polymers obtained. Therefore, we have made the NMR analyses of the polymers, taking into consideration the solubility in chloroform. On the one hand, no signals characteristic of terminal olefinic moiety in the monomers appeared in the ^{1}H NMR spectra, suggesting that excess monomers were eliminated from the polymers. On the other hand, δ value of –SiH– was shown near 4.68 ppm in the ^{1}H NMR spectrum of PMHS, but there was no peak near 4.68 ppm for all the polymers. For PMHS, the substitution degree can be determined by comparison of the integration of the Si–H signals to those of the Si–methyl groups. Disappearance of peak near 4.68 ppm indicated that all the Si–H bonds in PMHS were substituted via the hydrosilylation action, and the monomers were connected to the polysiloxane chains. Fig. 3 exhibits ^{1}H NMR spectrum of the representative polymer **Pe**. The grafting yield of **M1** and/or **M2**, and the polymer composition can also be calculated from the integration of different hydrogen protons. Because the peaks of –OC$\underline{H}_2$– were shown separately from other hydrogen protons in the ^{1}H NMR spectra, and only **M2** possesses the –OC$\underline{H}_2$– structure, the hydrogen protons on –OC$\underline{H}_2$– were chosen as basic arithmetical units in our case. The integration of 1 mole of hydrogen proton in the polymers was supposed as A_0, and the integration value of –OC$\underline{H}_2$– was measured as A_e in the ^{1}H NMR spectrum, thus the molar quantities of **M2** can be calculated as $A_e/(2A_0)$. There are 12 mole of phenyl hydrogen in 1 mole of **M2**, thus the molar quantities of phenyl hydrogen on **M2** can be calculated as $12A_e/(2A_0)$. The integration values of phenyl hydrogen were summed as A_p in the ^{1}H NMR spectrum, and total molar quantities of phenyl hydrogen are calculated as A_p/A_0. Because all the phenyl hydrogen atoms are originated from **M1** and **M2** components, the molar quantities of phenyl hydrogen from **M1** can be calculated as $[A_p/A_0 - 12A_e/(2A_0)]$. In addition, there are 16 mole of phenyl hydrogen in 1 mole of **M1**, thus the molar quantities of **M1** should be calculated as $[A_p/A_0 - 12A_e/(2A_0)]/16$. As a result, the molar ratio (R_{1-2}) of **M1**/**M2** in the side-chains should be calculated as

$$R_{1-2} = \mathbf{M1}/\mathbf{M2} = \{[A_p/A_0 - 12A_e/(2A_0)]/16\}/[A_e/(2A_0)] = (A_p - 6A_e)/(8A_e) \quad (1)$$

where A_e is the integration value of –OC$\underline{H}_2$–, and A_p is summarizing integration values of phenyl hydrogen in the polymers. Both A_e and A_p were measured from the ^{1}H NMR spectra.

Because all the side-chains in the polysiloxanes are **M1** and/or **M2** component, thus the mole fraction of **M1** component in all the side-chains ($\boldsymbol{V_1}$) should be calculated as

$$\boldsymbol{V_1} = \mathbf{M1}/(\mathbf{M1}+\mathbf{M2}) = (A_p - 6A_e)/(A_p - 6A_e + 8A_e) = (A_p - 6A_e)/(A_p + 2A_e) \quad (2)$$

and the mole fraction of **M2** component in all the side-chains ($\boldsymbol{V_2}$) is

$$\boldsymbol{V_2} = \mathbf{M2}/(\mathbf{M1}+\mathbf{M2}) = 8A_e/(A_p - 6A_e + 8A_e) = 8A_e/(A_p + 2A_e) \quad (3)$$

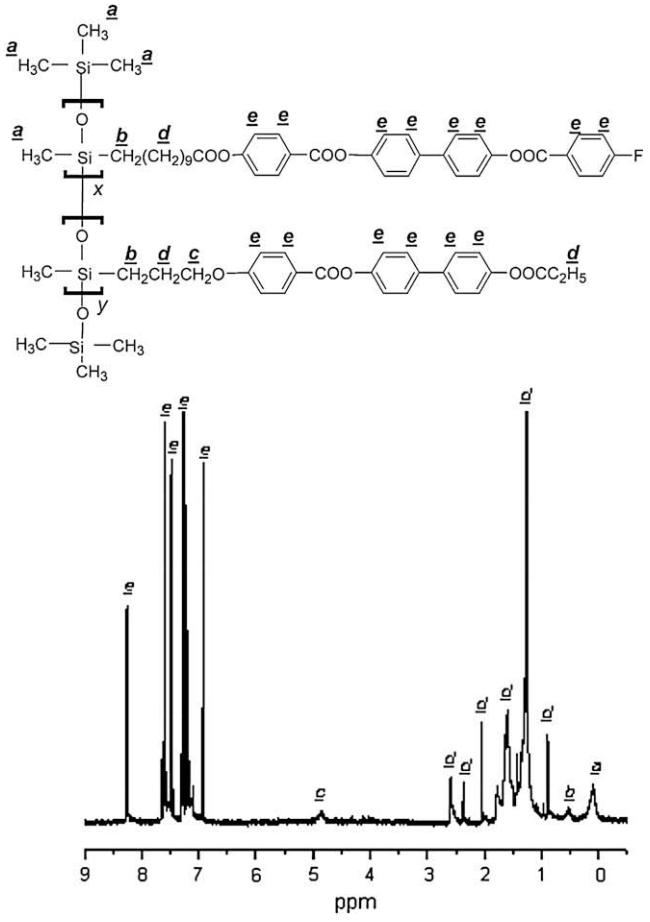

Fig. 3. ^{1}H NMR spectrum of the representative polymer **Pe**.

In addition, the molar quantities of Si–H bonds in PMHS were 35, and they were substituted totally by **M1** and/or **M2**. Thus the molar quantities of all the side-chains on 1 mole of polysiloxane are 35. According to both the mole fractions ($\boldsymbol{V_1}$ and $\boldsymbol{V_2}$) and the molecular weight of **M1** (and **M2**), molecular weights of the polysiloxanes should be determined. Therefore, the grafting yield, the polymer composition and molecular weights of the polymers could be calculated, which are listed in Table 1. It indicated that the M_n of the synthesized polymers increased slightly with the decrease of **M2** feed in polymerization.

Mass percentage of fluorine atom in the polymer systems obtained from EA measurements is listed in Table 1. Mass percentage of Fluorinated mesogens in the polymer systems can be determined by comparison of the atomic weight of fluorine and that of the fluorinated mesogenic units, as shown in Table 1. It indicated that the mass percentage of fluorinated mesogenic units increased with increase of monomer **M1** in the polymers.

3.2. Mesomorphic properties of monomers

Mesomorphic properties of these olefin monomers were studied using DSC, POM, and XRD. The study by DSC and POM enables us to determine the transition temperatures. Table 2 summarizes the thermal transition and corresponding enthalpy changes of monomers **M1** and **M2**, and DSC thermograms of the monomers are displayed in Fig. 4. The DSC curves of LC monomer **M1** with fluorinated mesogenic units showed a melting transition at 110 °C and mesogenic–isotropic phase transition at 130 °C on the second heating, as well as a isotropic–mesogenic transition at 125 °C and crystallization at 99 °C on the first cooling. The monomer **M2** exhibited melting point, clear point on the second heating at 203 °C and 241 °C respectively; and isotropic–mesogenic transition, crystallization on the first cooling at 214 °C and 189 °C respectively. The multi-benzene rings both lengthen the mesogens and make it more rigid, thus giving it a narrow temperature range of liquid crystalline phases for these two monomers.

Fig. 5 shows the typical nematic textures of monomers **M1** and **M2**. When **M1** was heated and cooled, droplet textures appeared as shown in Fig. 5a and b. For **M2**, Schlieren textures were observed between crossed polarizers, as displayed in Fig. 5c and d. Nematics

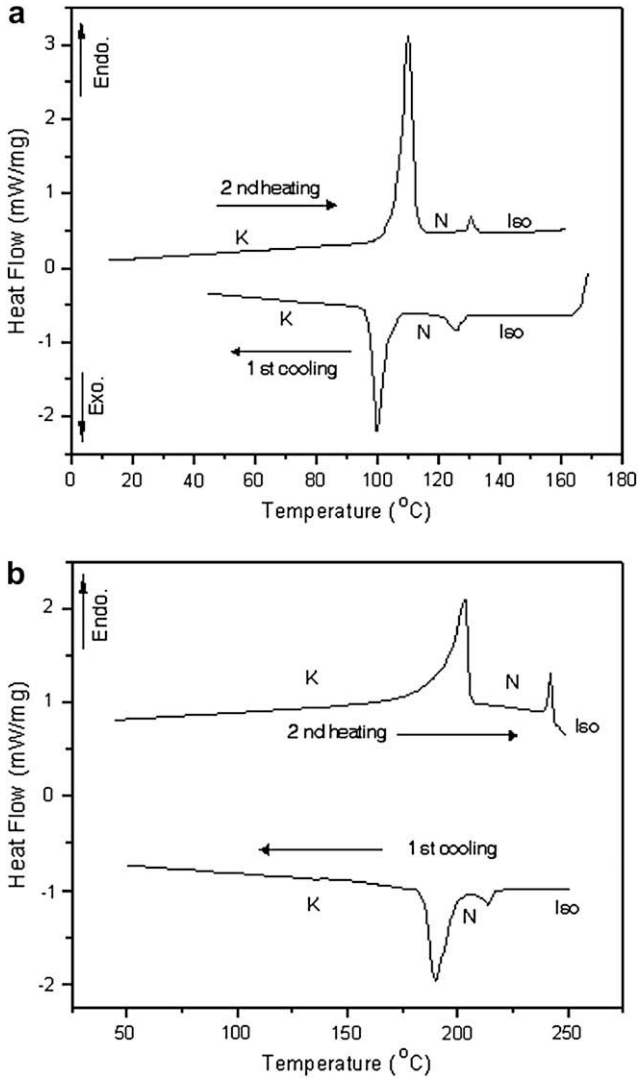

Fig. 4. DSC thermograms of monomers: (a) 4′-(4-undec-10-enoyloxy-benzoyloxy)-biphenyl-4-yl 4-fluoro-benzoate (**M1**); and (b) 4′-propionyloxy-biphenyl-4-yl 4-allyloxy-benzoate (**M2**).

Table 2
TGA, phase transitions and phase transition enthalpies for monomers and the series of polysiloxanes.

Sample	TGA			Phase transitions,[d] °C (corresponding enthalpy changes; J/g)
	T_d[a]	Inflection[b] (°C)	Residue[c] (%)	Heating
				Cooling
M1				C 110.1 (72.75) N 130.6 (2.63) I
				I 125.6 (4.87) N 99.6 (43.04) C
M2				C 203.7 (65.73) N 241.7 (10.07) I
				I 214.7 (1.54) N 189.7 (43.89) C
Pa	300.8	416.7	18.36	G 28.6 N 205.6 (6.43) I
				I 202.8 (0.46) N 20.8 G
Pb	311.9	409.9	24.92	G 27.0 N 198.0 (3.72) I
				I 178.7 (0.25) N 18.7 G
Pc	300.9	392.4	31.04	G 40.6 S_A 112.6 (0.47) N 199.6 (3.90) I
				I 178.4 (0.29) N 117.4 (0.19) S_A 19.4 G
Pd	318.4	385.7	32.3	G 41.0 S_A 112.0 (0.80) N 195.0 (2.66) I
				I 179.3 (0.24) N 107.3 (0.25) S_A 15.3 G
Pe	300.1	361.3	37.9	G 42.0 S_A 118.0 (2.19) N 191.0 (3.77) I
				I 169.9 (0.49) N 102.9 (0.05) S_A 18.9 G
Pf	319.1	–	39.35	G 43.3 S_A 126.3 (1.54) N 183.3 (0.74) I
				I 164.8 (0.52) N 97.8 (0.44) S_A 15.5 G

[a] Temperature of the samples at 5% loss weight.
[b] Inflection temperature of the samples between the two mass changes.
[c] Residue weight of the samples on heating to 600 °C.
[d] C, crystalline phase; G, glassy; N, nematic; S_A, smectic A; I, isotropic.

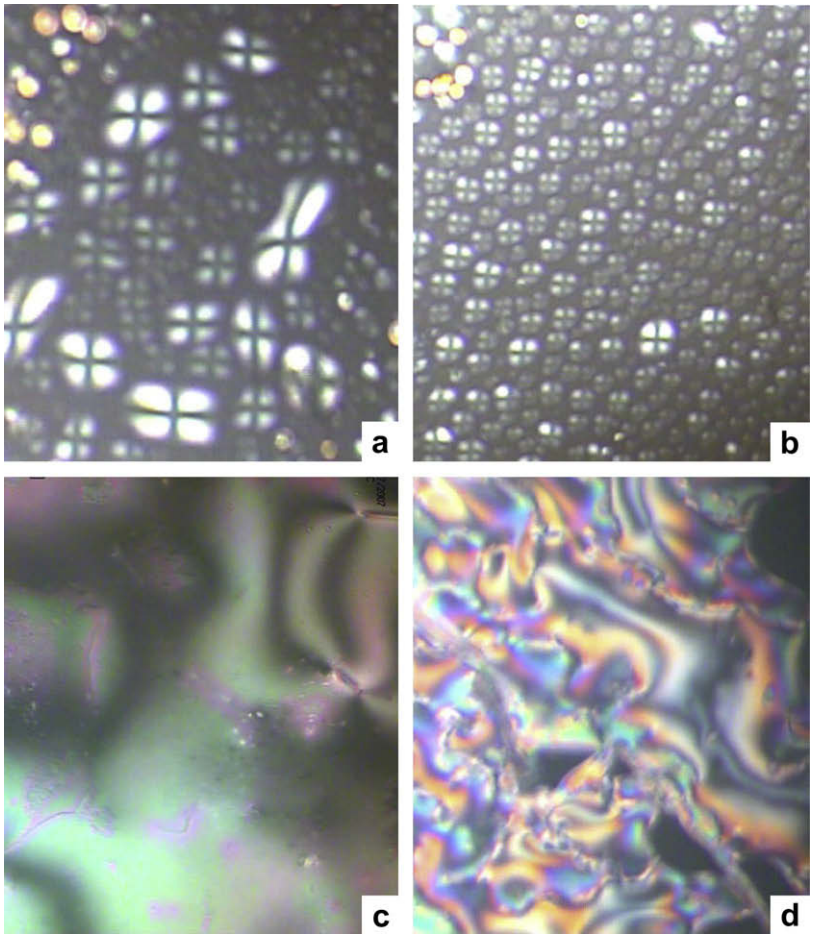

Fig. 5. Optical texture of the monomers (200×): (a) droplet texture of 4′-(4-undec-10-enoyloxy-benzoyloxy)-biphenyl-4-yl 4-fluoro-benzoate (**M1**) on heating to 115 °C; (b) droplet texture of **M1** on cooling to 124 °C; (c) Schlieren texture of 4′-propionyloxy-biphenyl-4-yl 4-allyloxy-benzoate (**M2**) on heating to 240 °C; (d) Schlieren texture of **M2** on cooling to 210 °C.

between untreated glass plates often orient with their director parallel to the substrates. If this orientation is not homogenous, but varies slowly in the plane of the substrate, so-called Schlieren textures are usually observed [32]. Furthermore, the powder X-ray diffraction pattern of the high-temperature phases of both **M1** and **M2** showed diffuse peaks in the wide-angle region, but no sharp peaks in the small-angle region appeared, suggesting no smectic layers. All these results indicated that both **M1** and **M2** displayed nematic mesophase.

3.3. Thermal analysis of polymers

TGA thermograms of the representative polymers are shown in Fig. 6, and the values are listed in Table 2. It suggested high thermal stability in consideration of greater than 300 °C of 5% weight loss temperatures (T_d) for all the polymers. T_d of **Pb**, **Pd** and **Pf** is higher than that of **Pa**, **Pc** and **Pe**. Because the bond energies of Si–O and Si–C bonds on polysiloxane main chains are much higher than those of C–C and C–O bonds, the polysiloxane main chains should be decomposed more difficultly than the side-chain component in the polymer systems. Therefore, T_d of the polymers would be mainly influenced by the side-chain structures of the polymers. On the one hand, rigidity should be increased with increase of fluorinated mesogenic units in the polymer systems from **Pa** to **Pf** because of introduction of more benzene ring, suggesting the increase of T_d. On the other hand, the polymer regularity would be decreased with introduction of more **M2** component into the polymers, resulting in decrease of T_d. Thus these opposed factors make T_d erratically, interpreting the reason why T_d of **Pb**, **Pd** and **Pf** is higher than that of **Pa**, **Pc** and **Pe**.

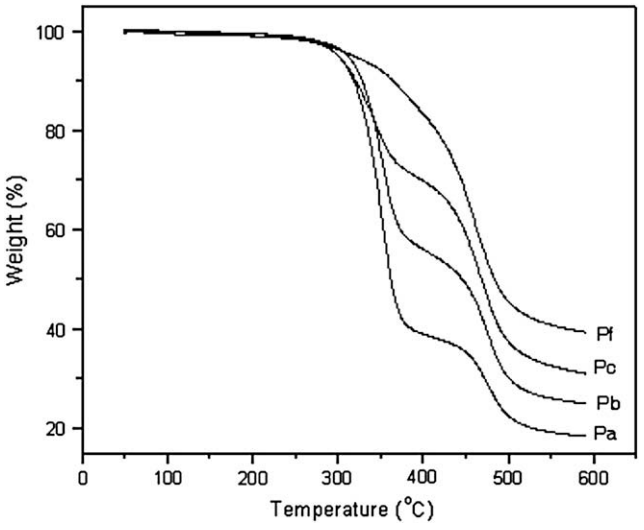

Fig. 6. TGA thermograms of representative polymers **Pa**, **Pb**, **Pc** and **Pf**.

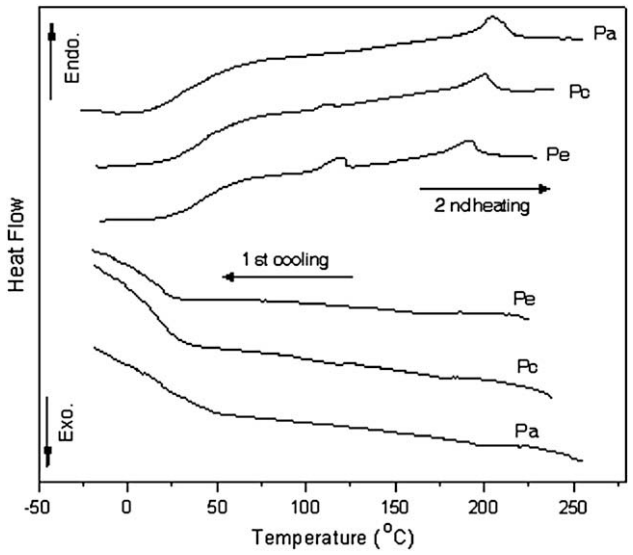

Fig. 7. DSC thermograms of representative polymers **Pa**, **Pc** and **Pe** on the second heating and on the first cooling cycles.

The samples **Pa**–**Pe** exhibited two mass changes, but the sample **Pf** showed only one mass change. The inflection temperature of the samples between the two mass changes decreased with increase of fluorinated mesogens in the polymer systems. Furthermore, for **Pf** which contained most fluorinated mesogenic units in the polymer systems, when there were no **M2** components in the polymers, no inflection temperature appeared. On the other hand, with increase of fluorinated mesogenic units in the polymer systems, the residue weight of the samples near 600 °C increased slightly from **Pa** to **Pf**, suggesting increased thermal stability. Therefore, all these TGA results suggested that the fluorinated mesogenic units influenced weight loss greatly.

For the polymers **Pa**–**Pf**, Table 2 exhibits the phase transitions and phase transition enthalpies obtained on the second heating and the first cooling scan. Representative DSC thermograms of the polymers on heating and cooling cycles are displayed in Fig. 7. For the polymers **Pa** and **Pb** which contain less fluorinated mesogenic units, they displayed glass transition temperature (T_g) and mesophase–isotropic phase transition temperature (T_i) on heating, and showed isotropic–mesomorphic phase transitions and mesomorphic–solid transitions on cooling. While for the polymers **Pc**, **Pd**, **Pe** and **Pf** which contain much more fluorinated mesogens, they displayed another phase transitions' temperature, i.e. smectic A–nematic mesophase transition temperature (T_{S-N}) besides T_g and T_i when they were heated.

Fig. 8 exhibits the relationship of transition temperatures (T_g, T_i and T_{S-N}) and fluorinated mesogenic units' component on heating cycles for the polymers. The T_g and T_{S-N} of polymers increased slightly with increase of fluorinated mesogenic units in the polymer systems, but T_i decreased slightly, suggesting that the mesomorphic temperature range became narrow with increase of fluorinated mesogenic units for the polymers. In addition, the molecular weight (M_n) of **Pa**–**Pf** increased with increase of fluorinated mesogenic units in the polymer systems, as shown in Table 2. For these kinds of side-chain liquid crystalline polymers, they are composed of flexible moieties (the polymer backbone, the flexible spacer groups and alkyl tails) and rigid moieties (mesogenic units and fluorinated mesogenic units), thus the interaction generating from fluorinated mesogenic units would influence mesophase behaviors of the polymers. For these disordered systems of the atactic siloxane polymers, the glass transition may be considered as a measure of the backbone flexibility. In our case, the polysiloxanes were graft copolymerized via hydrosilylation reaction with soft PMHS, one monomer (**M1**) containing undecylenate groups (long carbochains) and fluorinated mesogenic units, and another monomer (**M2**) containing allyloxy groups (short carbochains) and rigid mesogenic units. Thus the spacer groups and the rigid groups in the polysiloxane matrix are different for all the polymers. Accordingly, the backbone flexibility of the polymers is influenced mainly by two factors: the length of the flexible spacer and the rigid mesogenic units. When the fluorinated mesogenic units increased in the polymer systems, the flexible spacer increased as well, because they are all originated from the monomer **M1**. Because T_g of polymers increased slightly with more fluorinated mesogenic units in the polymer systems as shown in Fig. 8, it suggested that the backbone flexibility of these kinds of polymers should be predominated by the rigid fluorinated mesogenic units. On the other hand, T_i of polymers decreased slightly with more fluorinated mesogenic units in the polymer systems, indicating strong influence derived from interactions among fluorinated mesogenic units. Fluorine's small size, large electronegativity, low polarizability, and large fluorine–fluorine repulsion have also been proven to decrease the phase transition temperature from isotropic to nematic state [33].

In addition, the phase transition enthalpies of **Pa**–**Pf** are very different, as shown in Table 2. The effect factors include the samples, the apparatus and the measuring and test factors such as heat history, heating/cooling rate and furnace atmosphere. In our case, the sample characteristic becomes predominant factor due to the same measuring and test conditions for all the samples. Because polymers **Pa**–**Pf** were synthesized via hydrosilylation reaction between Si–H groups of PMHS and olefinic monomers **M1** and **M2**, the polymers possess different spacer groups and mesogens. The rigidity of fluorinated mesogenic units increased from **Pa** to **Pf** with increase of **M1** component that contains more benzene ring, leading to increase of phase transitions' enthalpy. At the same time, the order of the mesogens would be decreased due to different spacer groups and mesogens, resulting in decrease of phase transitions' enthalpy. As a result, the phase transitions' enthalpy of isotropic–mesogenic transition in Table 2 first decreases and later increases from **Pa** to **Pf**.

3.4. Texture analysis of polymers

The optical textures of the polymers were studied by use of POM with hot stage, and some representative optical textures are shown

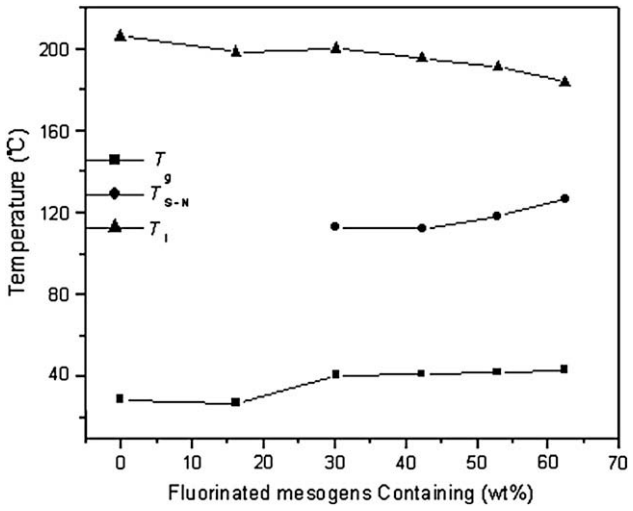

Fig. 8. Relationship between transition temperatures (T_g, glass transition; T_i isotropic transition; and T_{S-N}, mesophase transition from semectic A to nematic phase) and fluorinated mesogens containing in the polymers on the heating cycles.

in Fig. 9. The polymers displayed nematic and/or smectic textures when they were heated and cooled. For the sample **Pa** with no fluorinated mesogenic units, eyesight became bright and LC textures appeared when it was heated above 29 °C. The textures were seen obviously as the sample was heated continuously, and finally it exhibited textures with dark or bright lines, as shown in Fig. 9a. The thread-like textures of **Pa** were not as distinct as those of small molecule liquid crystals because of high viscosity. The thread-like texture of **Pa** disappeared at 205 °C, and the sample became isotropic state. When the isotropic melt was cooled, similar thread-like textures appeared gradually. For the sample **Pb** which contains a little fluorinated mesogenic units, when it was heated and cooled, analogous textures appeared, as shown in Fig. 9b. For the polymers **Pc**, **Pd**, **Pe** and **Pf** that contain more fluorinate mesogenic units, they showed similar smectic A broken focal conic texture textures on heating and cooling cycles (see Fig. 9c and d), but the textures were not as distinct as those of small molecule liquid crystals due to polymerization. We employed **Pc** as an example. When the sample **Pc** was heated, it showed broken focal conic texture, as displayed in Fig. 9c. The textures flowed slowly, and then some dark lines appeared, as the sample was heated continuously. The thread-like texture existed until the temperature of isotropic transition at 199 °C. These indicated that both smectic and nematic textures were exhibited when **Pc** was heated. When **Pc** was cooled from isotropic state, similar thread-like textures appeared gradually, and then broken focal conic textures appeared. The phase transition from the isotropic to SmA phase can easily be distinguished from that of Iso-N, that is, the direct transition to a fluid smectic phase was accomplished by the growth of batonnets. The batonnets were not observed here, suggesting that **Pc** showed firstly Iso-N transition.

3.5. X-ray diffraction analysis of polymers

The mesophase of the polymers was also characterized using X-ray diffraction analysis. The XRD data of all the polymers at 100 °C are summarized in Table 1, and representative XRD curves are exhibited in Fig. 10. A broad reflection at wide angles (associated with the lateral packings) and a sharp reflection at small angles (associated with the smectic layers) are separately shown by curves of polymers except for **Pa** and **Pb**. XRD curves of samples of **Pc**, **Pd**, **Pe** and **Pf** showed sharp and strong peaks at low angle ($2\theta \approx 2.5^{\circ}$) suggesting d-spacing near 35 Å, and a strong broad peak in wide angle ($2\theta \approx 20.4^{\circ}$) indicating d-spacing near 4.4 Å. Curves of **Pa** and **Pb** exhibited a diffuse reflection around 4.4 Å, which corresponds to the lateral spacing of two mesogenic side groups, but no reflection at 35 Å appeared, suggesting no smectic layer structure. When the polymer systems contain more fluorinated mesogenic units, curve of **Pc** displayed a weak reflection at 35.2 Å which corresponds to a weak smectic layer structure along with a diffuse reflection at 4.35 Å. Furthermore, the intensity of sharp reflections at low angle increased with increase of fluorinated mesogenic units in the polymers' systems for **Pc**, **Pd**, **Pe** and **Pf**, indicating strengthening smectic layer structure at 100 °C. But when they were heated, the sharp reflections at low angle disappeared gradually, finally showing similar curve of **Pa**. In general,

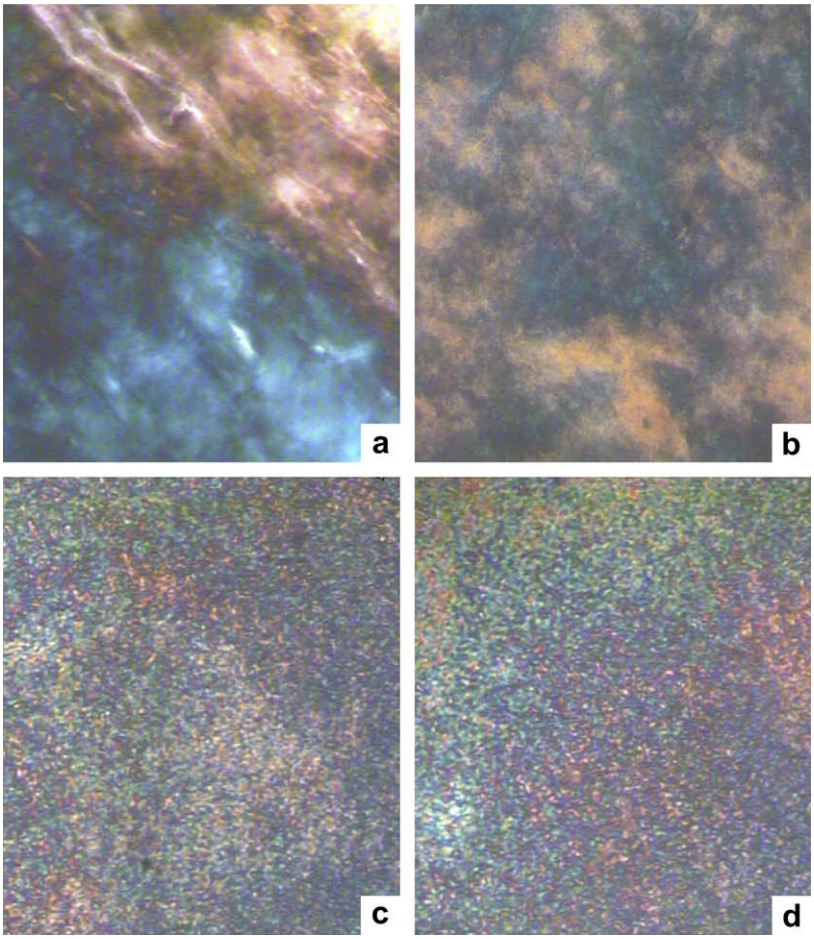

Fig. 9. Optical texture of the liquid crystalline polysiloxanes (200×): (a) **Pa** on heating to 178 °C; (b) **Pb** on heating to 166 °C; (c) broken focal conic texture of **Pc** on heating to 111 °C; (d) broken focal conic texture of **Pf** on cooling to 96 °C.

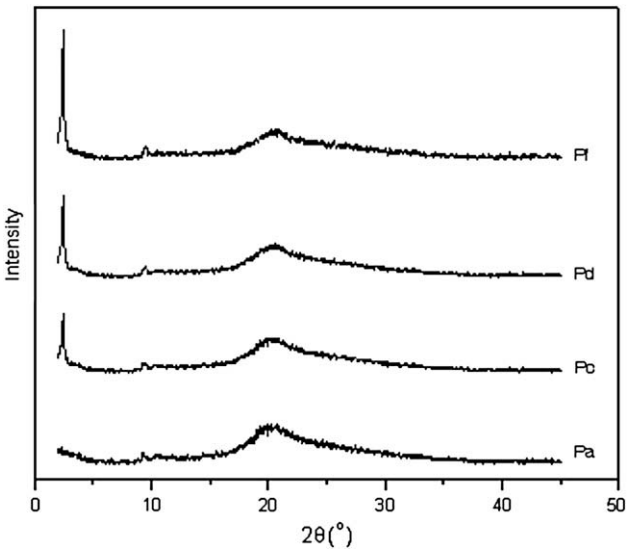

Fig. 10. Representative XRD curves of the series of polymers.

a sharp and strong peak at low angle ($1^\circ < 2\theta < 4^\circ$) in small angle together with a strong broad peak in wide angle can be observed for a smectic polymer structure. Therefore polymers **Pc**, **Pd**, **Pe** and **Pf** exhibited smectic A mesophase, but polymers **Pa** and **Pb** didn't display smectic A mesophase.

Because these liquid crystalline polymers are composed of flexible and rigid moieties, self-assembly and nanophase separation into specific micro-structures frequently occur due to geometric and chemical dissimilarities of the two moieties. For all the polysiloxanes, the flexible moieties are composed of siloxane main chains, soft alkyl spacer groups and alkyl tails, and the rigid moieties are comprised from mesogenic units and the fluorinated mesogenic units. Since the polymers were synthesized from monomers **M1** and **M2**, and **M1** comprises undecylenate groups and fluorinated mesogenic units which is different to the structure of **M2**, the soft spacer groups and the rigid groups are different for all the polymers. For the polymers **Pa** and **Pb** with less **M1** component in the polymer systems, the biphenyl ester mesogens originated from **M2** would be aligned regularly in the soft polymer matrix when the samples were heated and cooled, resulting in nematic mesophases. But the polymers **Pc**–**Pf** containing more **M1** moieties showed different features from **Pa**. With increase of **M1** component in the polymer systems, both the length of the flexible spacer and the fluorinated mesogenic units strengthened. Therefore, all these factors make **Pc**–**Pf** smectic structure, and the highly ordered smectic mesophases would be formed due to specific micro-structures. Furthermore, the incompatibility of the fluorinated mesogenic units with aliphatic, aromatic, polar molecular segments and siloxane matrix in the polymer systems could lead to a significant stabilization and even to modifications of smectic mesophases.

4. Conclusions

A series of side-chain LC polysiloxanes (**Pa**–**Pf**) bearing fluorinated mesogenic units were synthesized by use of poly (methylhydrogeno)siloxane and two LC monomers. The chemical structures and M_n were characterized with FTIR, ^{1}H NMR and EA. Phase behaviors of the fluorinated LC polysiloxanes were characterized using TGA, DSC, POM and XRD. The TGA results displayed that 5% weight loss temperatures were greater than 300 °C for all the polymers, and the residue weight near 600 °C increased slightly with increase of fluorinated mesogenic units in the polymer systems. The samples **Pa** and **Pb** showed nematic phase when it was heated and cooled. While the samples **Pc**, **Pd**, **Pe** and **Pf** exhibited both smectic and nematic phases. The T_g and T_{S-N} of polymers increased slightly with increase of fluorinated units in the polymer systems, but T_i decreased slightly. It suggests that the temperature range of mesophase became narrow with increase of fluorinated mesogenic units for all the polymers. The fluorophobic effect between the fluorinated mesogenic units and the polymer matrix results in decrease of the phase transition temperature from isotropic to nematic state. XRD curves of samples of **Pc**, **Pd**, **Pe** and **Pf** displayed sharp and strong peaks at low angle ($2\theta \approx 2.5^\circ$, *d*-spacing 35 Å) together with a strong broad peak in wide angle ($2\theta \approx 20.4^\circ$, *d*-spacing 4.4 Å). Curve of **Pa** and **Pb** exhibited a diffuse reflection at around 4.4 Å (corresponding to the lateral spacing of two mesogenic side groups), but no reflection at 35 Å (corresponding to a smectic layer structure) appeared. Furthermore, the intensity of sharp reflections at low angle increased with increase of fluorinated mesogenic units in the polymers' systems for **Pc**, **Pd**, **Pe** and **Pf**, indicating strengthening smectic layer structure. These results indicating that the longer spacer and the fluorophobic effect of fluorinated mesogenic units could lead to a significant stabilization and even to modifications of smectic mesophases.

Acknowledgments

The authors are grateful to Project 50873018 supported by National Natural Science Foundation of China, China Postdoctoral Science Foundation funded project, and Educational Science and Technology Program (Education Department of Liaoning Province) for financial support.

References

[1] Keith C, Dantlgraber G, Reddy RA, Baumeister U, Tschierske C. Chem Mater 2007;19:694–710.
[2] Kramer D, Finkelmann H. Macromol Rapid Commun 2007;28:2318–24.
[3] Knaapila M, Stepanyan R, Lyons BP, Torkkeli M, Monkman AP. Adv Funct Mater 2006;16:599–609.
[4] Guittard F, Givenchy ET, Geribaldi S, Cambon A. J Fluorine Chem 1999;100:85–96.
[5] Bunn CW, Howells ER. Nature 1954;174:549–56.
[6] Russell TP, Rabolt JF, Twieg RJ, Siemens RL, Farner BL. Macromolecules 1986;19:1135–43.
[7] Viney C, Twieg RJ, Russel TP, Depero LE. Liq Cryst 1989;5:1783–9.
[8] Andruzzi L, Apollo FD, Galli G, Gallot B. Macromolecules 2001;34:7707–14.
[9] Qin C, Rong G, Chen BQ, Wen JX. Chin J Chem 2006;24:99–102.
[10] Kirsch P, Tarumi K. Angew Chem Int Ed 1998;37:484–9.
[11] Bartmann E. Adv Mater 1996;8:570–3.
[12] Goto H, Dai X, Ueoka T, Akagi K. Macromolecules 2004;37:4783–93.
[13] You F, Paik MY, Hackel M, Kador L, Kropp D, Schmidt HW, et al. Adv Funct Mater 2006;16:1577–81.
[14] Chung TS, Ma KX, Cheng SX. Macromol Rapid Commun 2001;22:835–41.
[15] Crevoisier GD, Fabre P, Leibler L, Tence-Girault S, Corpart JM. Macromolecules 2002;35:3880–8.
[16] Krishnan S, Kwark YJ, Ober CK. Chem Rec 2004;4:315–30.
[17] Corpart JM, Girault S, Juhue D. Langmuir 2001;17:7237–44.
[18] Gopalan P, Andruzzi L, Li X, Ober CK. Macromol Chem Phys 2002;203:1573–83.
[19] Furukawa Y, Shin-ya S, Miyake H, Kishino H, Yamada M, Kato H, et al. J Appl Polym Sci 2001;82:3333–40.
[20] Wang J, Ober CK. Macromolecules 1997;30:7560–7.
[21] Beyou E, Babin P, Bennetau B, Dunogues J, Teyssie D, Boileau S. J Polym Sci Part A Polym Chem 1994;32:1673–9.
[22] Volkov VV, Plate NA, Takahara A, Kajiyama T, Amaya M, Murata Y. Polymer 1992;33:1316–23.
[23] Prescher D, Thiele T, Ruhmann R, Schulz G. J Fluorine Chem 1995;74:185–9.
[24] Goto H, Dai X, Narihiro H, Akagi K. Macromolecules 2004;37:2353–62.
[25] Bracon F, Guittard F, Givenchy ET, Cambon A. J Polym Sci Part A Polym Chem 1999;37:4487–96.
[26] Bubulak TV, Buchs J, Kohlmeier A, Bruma M, Janietz D. Chem Mater 2007;19:4460–6.
[27] Fujiwara M, Satoh K, Kondo S, Ujiie S. Macromolecules 2006;39:5836–42.
[28] Ding J, Du X, Day M, Jiang J, Callender CL, Stupak J. Macromolecules 2007;40:3145–53.

[29] Meng FB, Gao YM, Lian J, Zhang BY, Zhang FZ. Colloid Polym Sci 2008;286:873–9.
[30] Meng F, Lian J, Zhang B, Sun Y. Eur Polym J 2008;44:504–13.
[31] Milano JC, Robert JM, Vernet JL, Gallot B. Macromol Chem Phys 1999;200:180–90.
[32] Dierking I. Textures of liquid crystals. Weinheim: Wiley-VCH Press; 2003. p. 51–4.
[33] Ueda M, Noguchi Y, Sugiyama J, Yonetake K, Masuko T. Macromolecules 1992;25:7086–9.